Molecular Therapy
Oncolytics
Original Article

PSMA-Directed CAR T Cells Combined with Low-Dose Docetaxel Treatment Induce Tumor Regression in a Prostate Cancer Xenograft Model

Jamal Alzubi,[1,2] Viviane Dettmer-Monaco,[1,2] Johannes Kuehle,[3] Niko Thorausch,[4] Maximilian Seidl,[5] Sanaz Taromi,[6,7] Wolfgang Schamel,[4] Robert Zeiser,[6,8] Hinrich Abken,[9] Toni Cathomen,[1,2,8] and Philipp Wolf[8,10]

[1]Institute for Transfusion Medicine and Gene Therapy, Medical Center–University of Freiburg, Freiburg, Germany; [2]Center for Chronic Immunodeficiency, Medical Center–University of Freiburg, Freiburg, Germany; [3]Center for Molecular Medicine, University of Cologne, Cologne, Germany; [4]BIOSS Centre for Biological Signaling, University of Freiburg, Freiburg, Germany; [5]Institute of Clinical Pathology, Medical Center–University of Freiburg, Freiburg, Germany; [6]Department of Hematology, Oncology and Stem Cell Transplantation, Medical Center–University of Freiburg, Freiburg, Germany; [7]Faculty of Medical and Life Sciences, University Furtwangen, Campus Schwenningen, Villingen-Schwenningen, Germany; [8]Faculty of Medicine, University of Freiburg, Freiburg, Germany; [9]Department for Genetic Immunotherapy, Regensburg Center for Interventional Immunology, University of Regensburg, Regensburg, Germany; [10]Department of Urology, Medical Center–University of Freiburg, Freiburg, Germany

While chimeric antigen receptor (CAR) T cell immunotherapy targeting CD19 has shown remarkable success in patients with lymphoid malignancies, the potency of CAR T cells in solid tumors is low so far. To improve the efficacy of CAR T cells targeting prostate carcinoma, we designed a novel CAR that recognizes a new epitope in the prostate-specific membrane antigen (PSMA) and established novel paradigms to apply CAR T cells in a preclinical prostate cancer model. *In vitro* characterization of the D7 single-chain antibody fragment-derived anti-PSMA CAR confirmed that the choice of the co-stimulatory domain is a major determinant of CAR T cell activation, differentiation, and exhaustion. *In vivo*, focal injections of the PSMA CAR T cells eradicated established human prostate cancer xenografts in a preclinical mouse model. Moreover, systemic intravenous CAR T cell application significantly inhibited tumor growth in combination with non-ablative low-dose docetaxel chemotherapy, while docetaxel or CAR T cell application alone was not effective. In conclusion, the focal application of D7-derived CAR T cells and their combination with chemotherapy represent promising immunotherapeutic avenues to treat local and advanced prostate cancer in the clinic.

INTRODUCTION

Prostate cancer remains the second most frequent malignancy among men worldwide, with an estimated 1.1 million new cases per year. Moreover, with 307,000 deaths expected, it represents the fifth leading cause of cancer mortality.[1,2] Whereas primary tumors can be successfully treated by surgery or local radiation therapy, classical treatment options do not provide a curative treatment for advanced stages.[1] In this situation, immunotherapy with redirected T cells is thought to provide an alternative option. A rapidly emerging concept to treat cancer is based on the genetic engineering of T cells with chimeric antigen receptors (CARs), which bind tumor antigens or tumor-associated antigens in a human leukocyte antigen-independent manner. In general, CARs are composed of an extracellular domain harboring the antigen-specific single-chain variable fragment (scFv) antibody, a hinge domain, a transmembrane region, and intracellular signaling domains that activate engineered T cells upon antigen engagement. In clinically explored second-generation CARs, co-stimulatory domains generally derive from CD28 or 4-1BB.[3] Targeting hematological malignancies has shown great clinical success, particularly CD19 targeting CAR T cells to treat B cell malignancies.[4,5] For solid tumors, however, the potency of CAR T cell therapy is still low due to the immunosuppressive tumor microenvironment (TME) and accessibility of the tumor antigen,[6] among others.

Prostate-specific membrane antigen (PSMA) is considered an ideal target for antigen-redirected immunotherapy because it is expressed at the surface of prostate cancer cells,[7] present in all tumor stages, and shows an increased expression in androgen-independent and metastatic stages of the disease.[8–10] Several antibodies have been developed to target PSMA both for diagnostic purposes and for the development of antibody-based therapies,[11] such as J591,[12] 3D8,[13] D2B,[14] and 3/F11.[15] Many of these antibodies were the basis for the development of PSMA-targeting CARs,[16–19] of which some have entered clinical trials (e.g., ClinicalTrials.gov: NCT01140373, NCT01929239, and NCT03089203). However, the oncolytic potency of these PSMA CAR T cells is still uncertain. In particular, engineered

Received 4 March 2020; accepted 19 June 2020;
https://doi.org/10.1016/j.omto.2020.06.014.

Correspondence: Toni Cathomen, Institute for Transfusion Medicine and Gene Therapy, Medical Center–University of Freiburg, Hugstetter Strasse 55, 79106 Freiburg, Germany.
E-mail: toni.cathomen@uniklinik-freiburg.de
Correspondence: Philipp Wolf, Department of Urology, Medical Center–University of Freiburg, Breisacher Strasse 66, 79106 Freiburg, Germany.
E-mail: philipp.wolf@uniklinik-freiburg.de

T cells expressing first-generation CARs derived from 3D8[18] or J591[16,20] scFvs, respectively, showed low potency due to the low persistence of the CAR T cells. CAR T cell potencies improved when second- or third-generation CARs based on either D2B[21] or J591[17,19] scFvs were used. However, the anti-tumor activity remained moderate in tumor xenograft mouse models, and subjective responses were observed only when high CAR T cell doses or multiple infusions were applied.[18,20,21] Nonetheless, PSMA is still considered a good tumor-associated antigen. Although the salivary glands, proximal tubuli of the kidney, and the brush border of the duodenal columnar epithelium express PSMA,[22] CAR T cell-mediated "on-target/off-tumor" effects were not reported in any of the clinical trials that used 3D8-based CAR T cells.[23] Alternatively, some patients with metastatic castration-resistance prostate cancer developed severe cytokine release syndrome (CRS) in a clinical study with J591-based CAR T cells[24] that co-expressed a dominant-negative transforming growth factor β (TGF-β) receptor to render the CAR T cells insensitive to TGF-β.[25] While the reason for the reported CRS is not clear yet, the totality of the results indicate that prostate cancer is hard to treat by currently available CAR T cell strategies and that the development of potent anti-PSMA CAR T cells in combination with alternative treatment paradigms is highly warranted.

To generate a new PSMA-targeting CAR, we relied on the 3/F11 antibody-derived scFv D7. We previously reported that 3/F11 was less reactive to normal tissues as compared to J591.[18] Furthermore, D7 scFv was used to engineer *Pseudomonas* exotoxin A-based immunotoxins and bispecific anti-PSMA/anti-CD3 diabodies, which showed high and specific cytotoxicity against PSMA-expressing prostate cancer cells *in vitro* and *in vivo* in mice bearing human prostate tumors.[26–31] Another critical point in cell-based immunotherapies is that the engineered immune cells reach the tumor. We contemplated that focal injection of PSMA CAR T cells will ensure a high local intratumoral concentration of the engineered cells. Moreover, we speculated that low-dose chemotherapy with docetaxel (DTX), which is commonly used in combination with androgen deprivation therapy for the treatment of prostate cancer in a hormone-sensitive metastatic setting,[1] will slow down tumor growth and modify the TME, thereby enabling the CAR T cells to access and fight the cancer cells. In a recent study, the immunomodulatory potential of DTX was demonstrated: pretreatment of non-small-cell lung cancer with DTX elicited an enhanced expression of high-mobility group box 1 (HMGB1) from dying cells, which was followed by a higher secretion of the chemokine CXCL11 and an enhanced tumor infiltration of $CD8^+$ T cells.[32] Lastly, the CAR architecture and the CAR expression levels were reported to be major determinants of CAR T cell activity *in vivo*.[6,33–35]

In this study, we show that our new D7-based PSMA-targeting CAR can be expressed at high levels in transduced T cells, correlating with high antigen-specific activation and cytotoxicity of the resulting CAR T cells *in vitro*. *In vivo*, D7-based PSMA-targeting CAR T cells completely eradicated human prostate cancer xenografts in a mouse tumor model upon focal application. Furthermore, these CAR T cells significantly inhibited tumor growth in combination with a non-ablative dose of DTX chemotherapy upon intravenous (i.v.) application. These novel treatment paradigms represent promising immunotherapeutic avenues to treat local and disseminated prostate cancer in clinical applications.

RESULTS

Functional Validation of a New Anti-PSMA CAR

To target PSMA, we designed a novel second-generation CAR based on the D7 scFv, a modified immunoglobulin (Ig)G1 domain in the hinge region, which was shown to reduce potential interaction with the Fc receptor of innate cells,[36] and a modified CD28 co-stimulatory domain deficient in lymphocyte-specific protein kinase (LcK) binding, which results in an enhanced anti-tumor activity in the presence of regulatory T cells (Tregs).[37] For an initial validation of the D7-CAR, the scFvs 3D8[18] or J591[17] were cloned into the same CAR scaffold (Figure 1A; Figure S1A). Although almost 100% of Jurkat T cells were transduced with the corresponding γ-retroviral vectors in all three cases, D7-CAR28 was expressed at higher levels than 3D8- and J591-based CARs, respectively (Figure S1B), suggesting increased stability or improved intracellular transport of the D7-CAR. Antigen-specific activation of these CAR Jurkat cells (Figure S1C) by co-cultivation with PSMA-expressing prostate cancer cell lines LNCaP (programmed cell death ligand 1 $[PD\text{-}L1]^+$) or C4-2 ($PD\text{-}L1^-$) (Figure S2F) revealed a sound activation of D7-CAR- or J591-CAR-expressing Jurkat cells, respectively, but not of 3D8-CAR-expressing cells (Figure S1C). Next, primary D7-CAR and J591-CAR T cells were generated by retroviral transduction (Figure 1B) and evaluated in terms of cytotoxicity, cytokine release, antigen-specific activation, phenotype, exhaustion, and proliferation (Figures 1C–1E; Figures S1D–S1J). Of note, 3D8-CAR expression could not be detected following retroviral transduction of primary T cells (data not shown), mirroring the low expression levels in Jurkat cells. To assess cytolytic activity, these CAR T cells were co-cultured with C4-2 cells, LNCaP cells, or $PSMA^-$ DU145 cells at the indicated effector-to-target (E:T) ratios (Figure 1C; Figures S1D and S1E). D7-CAR T cells eliminated the prostate cancer cells at significantly lower E:T ratios than did the J591-CAR T cells (Figure 1C; Figure S1D), independent of the source of donor T cells or the PD-L1 expression status. As compared to the J591-CAR T cells, the higher cytotoxic activity of D7-CAR T cells correlated with higher interferon γ (IFN-γ) and granzyme A release, respectively (Figure 1D; Figure S1H), as well as higher antigen-specific activation (Figure 1E). Upon co-cultivation of these CAR T cells with C4-2 tumor cells at E:T ratios of 1:1, comparable T cell differentiation pattern (Figure S1I) and exhaustion profiles were detected (Figure S1J). When subjected to a repetitive antigen exposure challenge, D7-CAR T cells were enriched better than J591-CAR T cells (Figure S1F) even though the proliferation rate was comparable (Figure S1G). In conclusion, D7-CAR T cells outperformed J591-CAR T cells *in vitro* in terms of cytotoxicity, cytokine/granzyme release, and enrichment after repetitive exposure to antigen-positive target cells without having a negative impact on differentiation, exhaustion, and proliferation capacity.

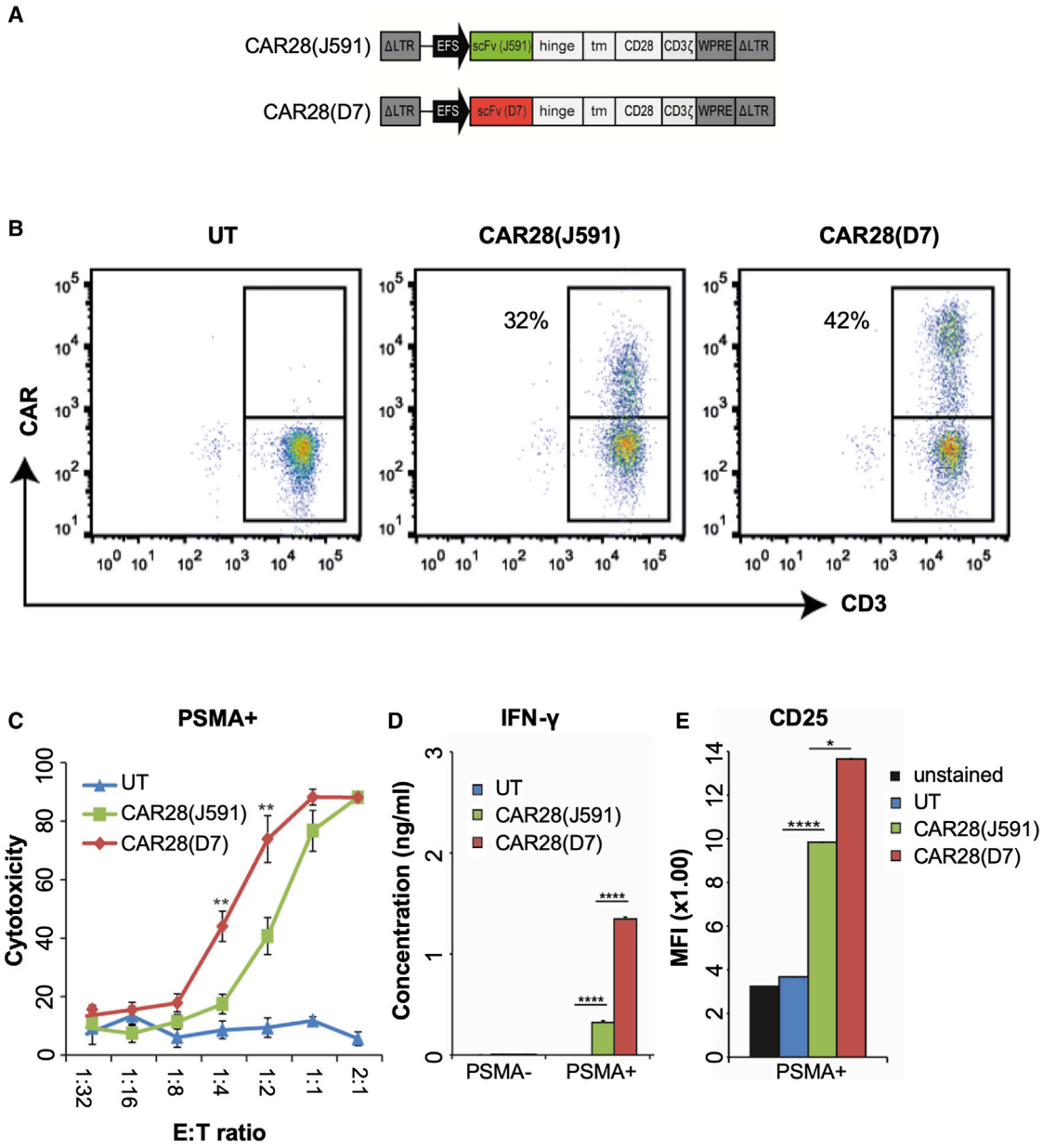

Figure 1. PSMA-Targeting CARs

(A) Schematic of CAR-expressing γ-retroviral vectors. See Figure S1A for details. (B) Evaluation of CAR expression. Activated T cells were transduced with γ-retroviral vector and stained with anti-human IgG antibody (CAR) and CD3. (C) Cytolytic activity. CAR T cells were co-cultured at the indicated E:T ratios with C4-2 cells ($PSMA^+/PD\text{-}L1^-$). Cytotoxicity was determined using a cell viability assay (n = 6). (D) Cytokine release. CAR T cells were co-cultured with $PSMA^+$ C4-2 or $PSMA^-$ Du145 cells, respectively, and the concentration of IFN-γ was determined in the supernatant (n = 3). (E) PSMA-mediated activation of CAR T cells. Activation of CAR T cells that were co-cultured with $PSMA^+$ C4-2 tumor cells was assessed by evaluating CD25 expression (n = 3). *p < 0.05, **p < 0.01, ****p < 0.0001. UT, untransduced cells; PSMA, prostate-specific membrane antigen; PD-L1, programmed cell death ligand 1; MFI, mean fluorescent intensity.

Impact of Co-stimulatory Domains on Activity of D7-CAR T Cells *In Vitro*

To assess the impact of the co-stimulatory signaling domain on D7-CAR T cell activity (Figure 2A), a CAR harboring the 4-1BB costimulatory domain (CAR41) was compared to CD28-based CAR T cells (CAR28) with regard to CAR expression levels, PSMA-specific activation, cytotoxicity, cytokine release, and antigen-specific differentiation. Both CARs were stably expressed upon γ-retroviral transduction (Figures S2A and S2B), and the resulting CAR T cells preserved a high percentage of early undifferentiated T cell subtypes

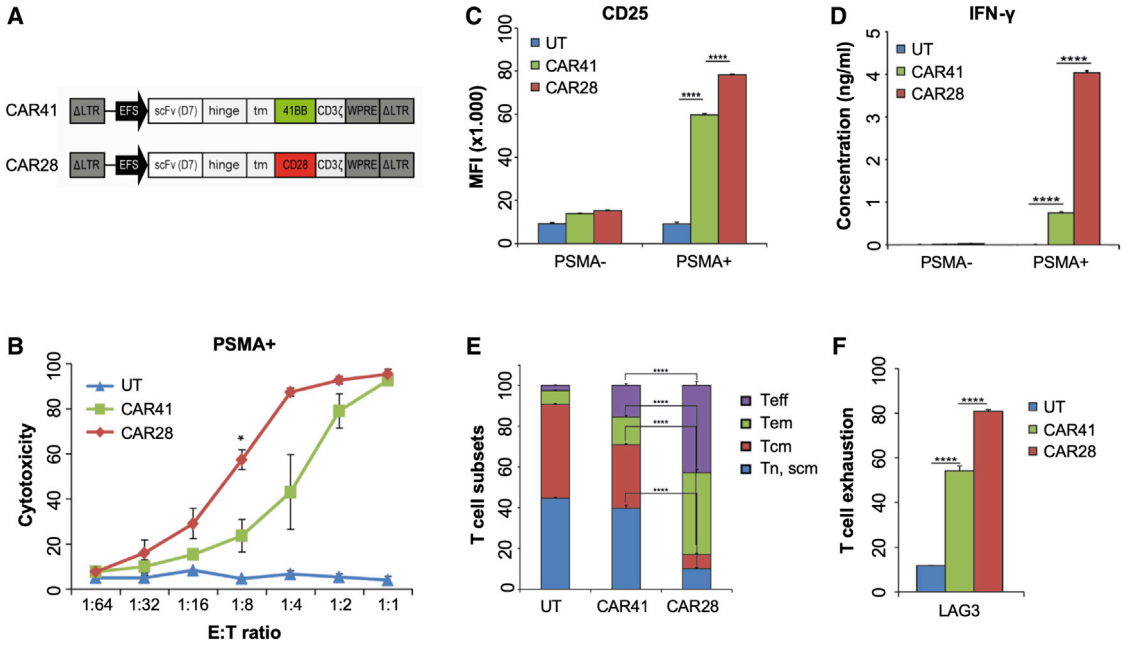

Figure 2. *In Vitro* Analysis

(A) Schematic of γ-retroviral vectors. See Figure S1A for details. Costimulatory domains were derived either from CD28 (CAR28) or 4-1BB (CAR41). (B) Cytolytic activity. CAR T cells were co-cultured at the indicated E:T ratios with PSMA$^+$ C4-2 tumor cells. Cytotoxicity was determined using a cell viability assay (n = 3). (C) PSMA-mediated activation of CAR T cells. CAR T cells were co-cultured with PSMA$^+$ (C4-2) or PSMA$^-$ (Du145) tumor cells. T cell activation was assessed by evaluating expression of CD25. Shown is mean fluorescent intensity (MFI, n = 6). (D) Cytokine release. CAR T cells were co-cultured with PSMA$^+$ (C4-2) or PSMA$^-$ (Du145) cells and IFN-γ in supernatant was measured (n = 3). (E) CAR T cell phenotype. CAR T cells were co-cultured with PSMA$^+$ tumor cells before the phenotype was assessed based on CD62L and CD45RA expression. Shown are the average percentages of the different T cell subsets (n = 3 or 4). (F) Exhaustion. CAR T cells were co-cultured with PSMA$^+$ tumor cells and the extent of T cell exhaustion was assessed by measuring expression of CD223 (LAG-3). Shown are the average percentages of LAG-3$^+$ cells (n = 3 or 4). *$p < 0.05$, ***$p < 0.001$, ****$p < 0.0001$. UT, untransduced T cells; Tn/Tscm, T cell naive or T stem cell memory; Tcm, T cell central memory; Tem, T cell effector memory; Teff, T cell effector; LAG-3, lymphocyte activation gene 3.

at the end of the expansion phase (Figures S2C and S2D). Interestingly, CAR28 was expressed at higher levels at the cell surface (Figure S2A), although total CAR expression was greater for CAR41 (Figure S2B). This might be due to a more efficient intracellular transport of CAR28 to the cell surface.

While both CARs mediated killing in a PSMA-dependent manner (Figure S2E), CAR28 T cells eliminated antigen-positive prostate cancer cells at a lower E:T ratio in a short-term *in vitro* assay than did CAR41 T cells (Figure 2B). As compared to CAR41 T cells, co-cultivation of CAR28 T cells with PSMA$^+$ tumor cells induced a higher upregulation of activation markers CD25 (Figure 2C) and CD69 (Figure S3A). Analysis of the supernatants revealed that CAR28 T cells secreted significantly higher amounts of IFN-γ (Figure 2D) and granzyme B (Figure S3B) than did CAR41 T cells when co-incubated with PSMA$^+$ tumor cells. The percentages of differentiated T cell subsets, such as effector memory and terminally effector T cells, was significantly higher for CAR28 T cells in comparison to CAR41 T cells (Figure 2E; Figure S3C), and CAR28 T cells were found to be more exhausted, as indicated by upregulated LAG3 (Figure 2F; Figure S3D). In summary, and in agreement with published data,[38] the co-stimulatory domain had a major impact on activity and phenotype of D7-CAR T cells.

Elimination of Prostate Cancer Xenografts upon Focal Application of CAR T Cells

In order to explore the *in vivo* potency of the CAR T cells, a xenograft mouse model was used. To this end, C4-2^{luc+} cells were subcutaneously applied into the right flank of the animals. When tumors reached a mean volume of 70 mm^3, one dose of 5×10^6 CAR28 T cells, CAR41 T cells, or non-transduced T cells, respectively, were intratumorally (i.t.) injected and changes in tumor volume were monitored by *in vivo* bioluminescence imaging (BLI) until day 22 (Figure 3A). In line with the *in vitro* data, CAR28 T cell treatment was more efficacious than CAR41 T cell-based therapy. Treatment with CAR28 T cells eliminated the tumors in five out of five mice between day 3 and day 8 (Figures 3B and 3C), with four out of five mice maintaining complete remission (CR) until the end of the experiment (Figure 3D). Treatment with CAR41 T cells resulted in one case each of CR and partial remission (PR), whereas mice injected with non-transduced T cells did not respond to treatment. The calculation of the area under the curve (AUC), which considers the temporal course of tumor growth, confirmed the increased antitumor activity of CAR28 T cells compared to CAR41 T cells (Figure S4A). In conclusion, focal injection of CAR T cells may be a promising approach to treat local prostate cancer.

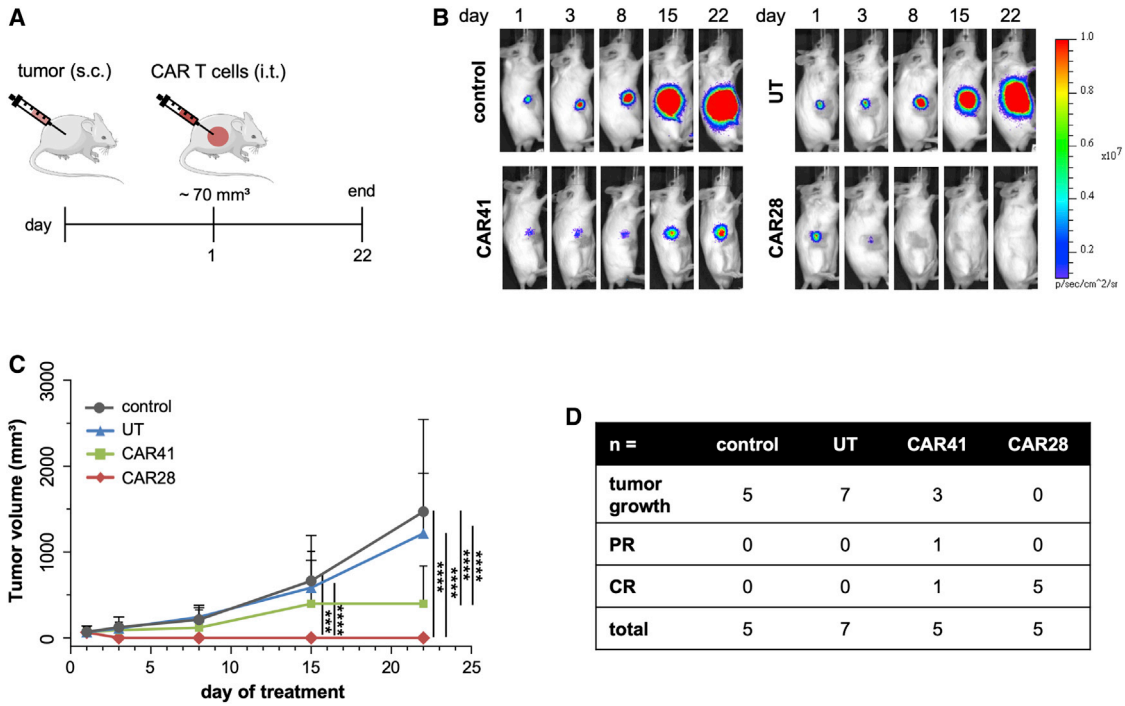

n =	control	UT	CAR41	CAR28
tumor growth	5	7	3	0
PR	0	0	1	0
CR	0	0	1	5
total	5	7	5	5

Figure 3. Focal CAR T Cell Therapy

(A) Schematic of experimental setup. 5- to 6-week-old SCID mice were injected subcutaneously (s.c.) with 1.5×10^6 PSMA$^+$ C4-2^{luc+} tumor cells. When tumors reached ~70 mm^3, mice were injected intratumorally (i.t.) with a single dose of 5×10^6 CAR28 (n = 5) or CAR41 (n = 5) T cells (day 1 of treatment). As controls, mice were left untreated (control, n = 6) or injected with untransduced T cells (UT, n = 7). (B) *In vivo* imaging. Shown are representative *in vivo* bioluminescence images (BLIs) of mice in different treatment groups. (C) Quantification of tumor size. Tumor volumes were determined on days 1, 3, 8, 15, and 22 of treatment. (D) Summary. Shown is antitumor response in different treatment groups. CR, complete response; PR, partial response. ***p < 0.001, ****p < 0.0001, by unpaired t test.

Combination Therapy with DTX Controls Prostate Cancer Xenograft Growth upon i.v. CAR T Cell Application

Using the same experimental conditions as above, one i.v. injection of 5×10^6 CAR T cells did not affect tumor growth during the course of the experiment (Figure S4B), although the CAR T cells reached the tumor site as detected by *in vivo* imaging (Figure S4C). We conjectured that treatment with the chemotherapeutic agent DTX would render the tumors more susceptible to CAR T cell therapy by reducing tumor growth and/or altering the TME. For combination treatment, mice bearing C4-2^{luc+}-derived large tumors (mean tumor volume of 150–200 mm^3) were injected intraperitoneally (i.p.) with two cycles of DTX at days 1 and 2 of treatment, followed by i.v. injection of a single dose of 5×10^6 CAR T cells on day 8. Control groups were treated with DTX alone or left untreated (Figure 4A). Concurring with our approved animal protocol, tumor growth was monitored by BLI until day 22. For ethical reasons, some mice bearing large and aggressive tumors had to be euthanized before the end of the experiment. Treatment with DTX alone did not considerably affect tumor growth (Figures 4B and 4C; Figure S4D). While the combination of DTX with CAR41 T cell therapy had some effect on tumor growth, the combination of DTX with CAR28 T cells led to a significant reduction in tumor growth from day 17 on (Figures 4B and 4C). While a TME hardly fully develops in the immunodeficient mouse background, our histological analysis of the tumors indicated the formation of some features of a primitive TME, as indicated by the presence of connective tissue and tumor stroma with low cellular density and some infiltrated macrophages (Figures 5A and 5B). The application of DTX chemotherapy induced tumor damage marked by vacuolization and nuclear condensation of the tumor cells. Moreover, a high proportion of tumor cells with metaphase arrest was found, which can be attributed to the cell cycle inhibitory effect of DTX. Compared to control, the TME showed a higher cellularity with an infiltration of innate immune cells, accompanied by some stromal edema (Figures 5C and 5D). In tumors from mice treated with combination therapy, extensive damage of the tumor marked by necrotic tumor cells on the tumor stroma border was found. The TME was marked by stromal edema and infiltration of CD3$^+$ CAR T cells. These characteristics were less pronounced in tumors treated with DTX and CAR41 T cells (Figures 5E and 5F) as compared to tumors treated with DTX and CAR28 T cells (Figures 5G and 5H), which was in line with a higher number of infiltrating CD3$^+$ cells. In summary, we engineered CAR T cells that completely eradicated prostate cancer xenografts after a single focal application. Moreover, in combination with low-dose, non-ablative DTX chemotherapy, significant inhibition of tumor growth was achieved after systemic application of PSMA-targeting CAR28 T cells.

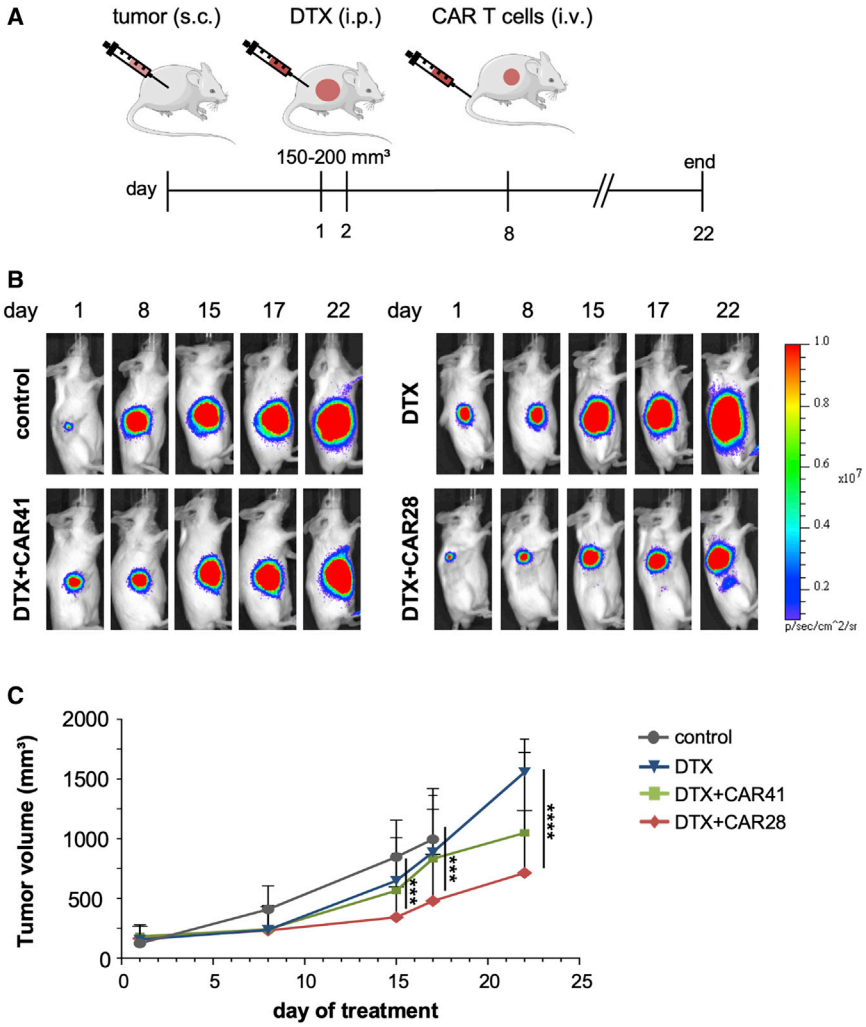

Figure 4. Combination of Chemotherapy with Systemic Application of CAR T Cells

(A) Schematic of combination therapy. 5- to 6-week-old SCID mice were injected subcutaneously (s.c.) with 1.5 × 10^6 C4-2^{luc+} tumor cells. When tumors reached a mean tumor volume of 150–200 mm^3, mice were treated intraperitoneally (i.p.) with two cycles of DTX (6 mg/kg body weight [bw]) at days 1 and 2 of treatment. At day 8, mice received one i.v. dose of 5 × 10^6 CAR28 (n = 9) or CAR41 T cells (n = 8). As controls, mice were injected with DTX alone (DTX, n = 9) or left untreated (control, n = 8). (B) *In vivo* monitoring. Shown are representative *in vivo* bioluminescence images (BLIs) of mice in different treatment groups. (C) Quantification of tumor size. Tumor volumes were determined on days 1, 8, 15, 17, and 22 of treatment. ***$p < 0.001$, ****$p < 0.0001$, by unpaired t test.

DISCUSSION

The great success of CAR T cells to treat certain hematological malignances could not be transferred to solid tumors thus far. A main reason for this failure might be the TME that includes various kinds of immune cells, fibroblasts, and an extracellular matrix. Any of these factors could either intrinsically or physically inhibit the migration and/or activity of CAR T cells,[6] suggesting that current CAR T cell therapies may not be successful without additive therapeutic interventions, such as checkpoint blockade or chemotherapy. We hypothesized that the focal administration of CAR T cells or their application in combination with chemotherapy may pave the way to a more successful treatment of solid tumors. To this end, we designed novel D7 scFv-based CARs to target PSMA and validated these CAR T cells in a xenograft mouse model. We demonstrate that local application of anti-PSMA CAR T cells led to complete eradication of prostate cancer, while systemic application of CD28-based CAR T cells significantly inhibited tumor growth when combined with low-dose DTX chemotherapy.

Our combined *in vitro* and *in vivo* data confirmed that D7-based CARs mediated high antigen-specific activation and cytotoxicity of the engineered T cells. The observed difference in comparison to previously reported PSMA-CARs in terms of efficacy may be found in the binding properties of the used scFvs and/or the heightened CAR expression, as previously shown for CARs targeting mesothelin or CD22.[33,39] We previously demonstrated that the D7 scFv binds PSMA with high affinity and specificity.[15] Moreover, we showed that its parental 3/F11 antibody recognizes a different extracellular epitope in PSMA than J591.[15,40] It is therefore interesting to speculate that the high *in vitro* and *in vivo* efficacy of D7-based PSMA CAR T cells is based on optimal positioning of the CAR to recognize the target epitope.

Both CD28- and 4-1BB-based CAR T cells showed promising clinical results against B cell malignancies, albeit with different tumor-killing kinetics: inclusion of CD28 appears to mediate faster tumor reduction, whereas 4-1BB promotes T cell persistence.[4,5,38] Our results are in line with these studies for lymphoid malignancies and showed that 4-1BB-based PSMA-CARs mediated an attenuated activation of the CAR T cells, resulting in less differentiation and less exhaustion upon antigen-specific stimulation.[6] Although our animal protocol did not allow us to assess long-term effects, CD28-bearing PSMA-CAR T cells induced complete tumor eradication upon local application. PSMA-targeting CAR T cells were previously applied i.t. with ~50% of treated mice showing CR upon injection of two doses of J591-based CAR T cells.[20] This underlines the excellent performance of the new D7-based CAR for focal therapy. A local therapy could be highly attractive to treat early stage prostate cancer as it will avoid, or at least reduce, systemic-associated toxicities related to CAR T cell activation at "off-tumor" tissues that express the PSMA antigen at lower levels. It will also enable CAR T cells to bypass the TME, so overcoming the challenge of CAR T cell trafficking to and infiltration of the tumor.[41]

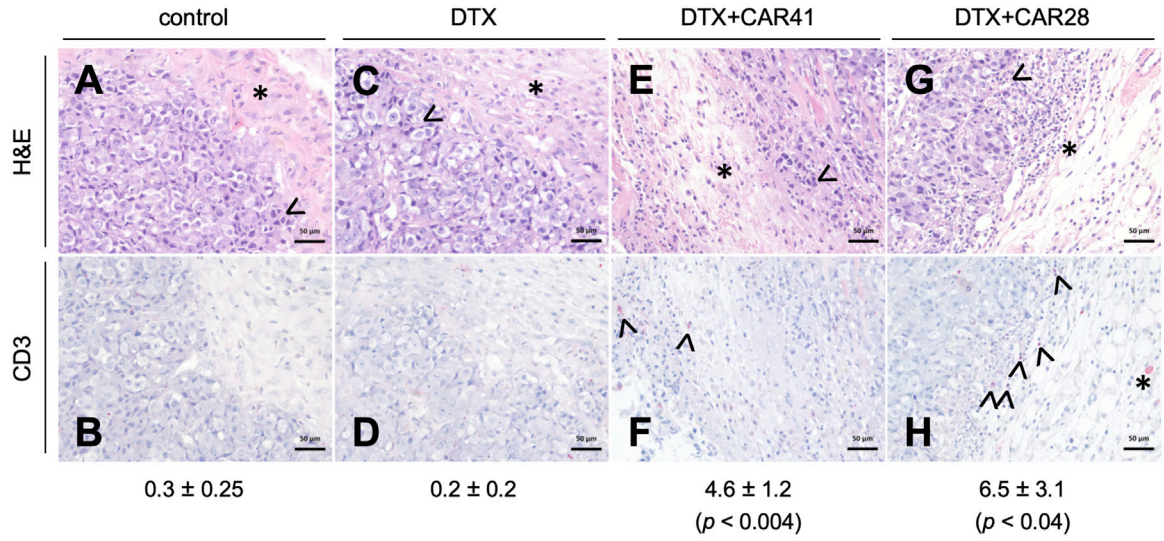

Figure 5. Histology

At the end of the combined docetaxel (DTX) and CAR T cell therapy, tumor slices of indicated groups were subjected to histopathological analysis by hematoxylin and eosin (H&E) staining (A, C, E, and G) or immunohistochemical analysis using anti-human CD3 that highlights human $CD3^+$ T cells in red (B, D, F, and H). (A and B) Untreated group (control) with few nuclear condensations (arrowhead, exemplary) of tumor cells near the tumor margin, low cellular density in the tumor microenvironment (TME), consisting of connective tissue with few macrophages (asterisk), and absence of $CD3^+$ T cell infiltrates. (C and D) DTX-treated group with nuclear condensations and cellular vacuolization but higher cellularity in the TME due to infiltration of monocytes and neutrophil granulocytes (asterisk), accompanied by stromal edema, and absence of $CD3^+$ T cells. (E and F) Combination therapy group (DTX and CAR41 T cells) with presence of TME with high stromal edema and stroma cellularity due to increased monocytes, macrophages, and lymphocytes infiltrating the connective tissue (asterisk in E), accompanied by tumor necrosis at the tumor-stroma border (arrowhead in E), and few infiltrating $CD3^+$ T cells in the TME (arrowheads in F). (G and H) Combination therapy group (DTX and CAR28 T cells) with presence of TME with high stromal edema and stroma cellularity (asterisk in G), accompanied by tumor necrosis zone (arrowhead in G), and high amount of infiltrating $CD3^+$ T cells (arrowheads in H) and macrophage with $CD3^+$ cytoplasm (asterisk in H). The average numbers ± standard error of the mean of infiltrating CD3 cells per tumor slice is indicated below. p values are indicated for comparison between the DTX group versus the DTX+CAR41 or DTX+CAR28 groups.

In agreement with previous publications,[21,42] the D7-CAR T cells were not able to eradicate large solid tumors upon systemic application. However, two cycles of non-ablative low-dose chemotherapy were sufficient to modify the TME, thereby allowing the PSMA-targeting CAR T cells to infiltrate the tumor and control tumor growth upon a single dose of i.v. administration. It will be interesting to assess whether DTX treatment induces the secretion of $CD8^+$ T cell-attracting cytokines from prostate cancer cells, as previously reported for non-small-cell lung cancer.[32] Furthermore, it will be attractive to combine DTX treatment with "enhanced" CAR T cells[43,44] by knocking out, for example, genes coding for inhibitory receptors, such as PD-1,[45] CTLA4,[46] LAG3,[47] or the T cell receptor,[48] or to introduce simple modifications to the CAR scaffold that have proven to increase safety and efficacy of CAR T cells in preclinical models of leukemia and lymphoma.[34,35]

In conclusion, we developed a novel D7-based anti-PSMA CAR that demonstrated excellent *in vitro* and *in vivo* activity. Notably, the CAR T cells were able to completely eradicate prostate cancer upon focal application and control tumor growth in combination with non-ablative low-dose chemotherapy upon systemic application. These preclinical data are encouraging and are enough to move forward to the clinic.

MATERIALS AND METHODS

Culturing of Prostate Cancer Cells

Prostate cancer cell lines were grown in RPMI 1640 medium (Gibco) supplemented with penicillin (100 U/mL), streptomycin (100 mg/L), and 10% fetal calf serum (FCS, Biochrom) at 37°C in a humidified atmosphere of 5% CO_2. For *in vivo* tumor establishment and bioluminescence imaging, C4-2 cells were transduced with a lentiviral vector encoding firefly luciferase and a neomycin resistance gene as previously described.[49]

CAR Design and Preparation of γ-Retroviral Vectors

Second-generation anti-PSMA CARs were cloned into the backbone of a self-inactivating γ-retroviral vector[50] by conventional cloning. All CARs are under control of the EFS promotor and contain an optimized hinge domain[36] and a CD3ζ intracellular signaling domain. The various CARs harbor scFv domains derived from monoclonal antibodies 3D8 (US2017/0232070 A1; SEQ ID 21), J591 (WO 2009/017823 A2), or D7.[15] The CAR28 scaffolds harbor the transmembrane domain of CD28 and the CD28 co-stimulatory domain with a modified LcK binding moiety.[37] The CAR41 scaffold contains a CD8α transmembrane domain and the 4-1BB co-stimulatory domain. Retroviral vectors were generated as previously described.[51]

Biological titers were determined by transducing Jurkat T cells, followed by staining of the transduced cells with anti-human IgG to determine CAR^+ cells.

Generation and Culturing of CAR T Cells

CAR-transduced Jurkat cells were expanded in RPMI complete medium (RPMI 1640 medium [Gibco] supplemented with 10% FCS [Biochrom], penicillin [100 U/mL], streptomycin [100 mg/L], and 10 mM HEPES buffer [Sigma-Aldrich]). Primary CAR T cells were generated from peripheral blood mononuclear cells (PBMCs) as described before[52] with modifications. In short, PBMCs were isolated from leukocyte reduction system (LRS) chambers obtained from the Blood Donation Center (informed consent of donors) of the Medical Center using phase separation (Ficoll, Sigma-Aldrich) and frozen in liquid nitrogen until used. For generation of CAR T cells, PBMCs were thawed in RPMI complete medium, activated with anti-CD2/CD3/CD28 antibodies (ImmunoCult, STEMCELL Technologies), and cultured with RPMI complete medium supplemented with cytokine cocktail (100 U/mL of IL-2, 25 U/mL of IL-7, and 50 U/mL of IL-15; all Miltenyi Biotec) for 3 days before transduction with γ-retroviral constructs with a dose of 50–300 transducing units/cell. Transduced cells were cultured in RPMI complete medium supplemented with 5 μg/mL of protamine sulfate (Sigma-Aldrich) and 1,000 U/mL of IL-2, 25 U/mL of IL-7, and 50 U/mL of IL-15 on poly-D-lysine (PDL, Sigma-Aldrich)-coated wells. After 1 day, medium was changed and cells were expanded for 9–12 days in RPMI complete medium supplemented with cytokine cocktail before being frozen in liquid nitrogen until further use.

Phenotyping of CAR T Cells

To determined transduction efficiency, surface CAR expression was evaluated by flow cytometry (FACSCanto II or Accuri, BD Biosciences) by staining transduced cells with anti-human IgG-phycoerythrin (PE) (SouthernBiotech) and CD3-allophycocyanin (APC) (Miltenyi Biotec), respectively. For phenotyping, CAR-transduced cells were stimulated with $PSMA^+$ tumor cells (C4-2 or LNCaP) for 24 h at an E:T ratio of 1:1, before cells were harvested and evaluated. Activation was evaluated based on the expression of CD69 or CD25 (CD69-APC, clone CH4; CD25-PE, clone 3G10; both Thermo Fisher Scientific). T cell subsets were determined by staining cells with anti-human CD62L-Brilliant Violet 421 (BV421) (BD Biosciences), anti-human CD45RA-fluorescein isothiocyanate (FITC) (BioLegend), anti-human CD3-APC/H7 (BD Biosciences), and anti-human IgG-PE (SouthernBiotech). To determine exhaustion, cells were stained with anti-human CD279-FITC (PD-1, BD Biosciences), anti-human CD223-eFluor 710 (LAG-3, BD Biosciences), anti-human CD3-APC/H7, and anti-human IgG-PE.

Cytokine Release

CAR T cells were co-cultured with $PSMA^+$ C4-2 tumor cells for 48 h at an E:T ratio of 1:1 in RPMI complete medium without cytokines. Supernatants were collected and evaluated by a multiplexed cytometric bead array (CBA, BD Biosciences) according to the manufacturer's recommendations.

Cytolytic Activity of CAR T Cells

To determine the cytotoxic potential of CAR T cells, the viability of target cells was determined using the XTT (2,3-bis-(2-methoxy-4-nitro-5-sulfophenyl)2*H*-tetrazolium-5-carboxanilide) assay as described previously.[53] In short, to determine cell viability as a function of metabolic activity, 100 μL of medium was removed and replaced with 100 μL/well of XTT solution (Sigma-Aldrich) and cells were incubated at 37°C. Colorimetric changes were quantified using an ELISA reader (Infinite F50, Tecan) at 450 nm. Cytotoxicity is indicated as 100% minus the percentage of viable cells, which was calculated according to the equation $(OD_{E+T} - OD_{E\ only})/(OD_{T\ only} - OD_{medium\ only})$, where OD indicates optical density, E represents effector cells (CAR T cells), and T represents target cells (tumor cells).

In Vivo Evaluation of CAR T Cells

Male severe combined immunodeficiency (SCID) CB17/lcr-*Prkdc*^{scid}/Crl mice (5–6 weeks old, 20-25 g) were purchased from Janvier Labs (Saint-Berthevin, France) and kept under sterile and standardized environmental conditions. All experiments were carried out according to the animal protection law and ARRIVE guidelines with permission from the responsible local authorities. For tumor establishment, 1.5×10^6 C4-2^{luc+} cells diluted in 50% Matrigel/PBS (Collaborative Biomedical Products) were injected subcutaneously into the right flank of the animals. Tumor growth was monitored by palpation and BLI. To this end, 150 μg/kg of luciferin (BioSynth AG) were injected i.p. into the animals and BLI was done 10–30 min after injection under anesthesia using the *in vivo* imaging system (IVIS) 200 (Xenogen VivoVision). Tumor volumes were calculated from BLI using the software Living Image 3.0 and the formula $V = (d2 \times D)/2$, where d was the smaller diameter and D the larger diameter of the tumor. When tumors reached a mean volume of about 70 mm^3, mice were injected either i.t. or i.v. with one dose of 5×10^6 CAR28 T cells (n = 5) or CAR41 T cells (n = 5), untransduced T cells with a dose matching the final total cells in the CAR-treated groups (UT, n = 5–7), or left untreated (control, n = 6). For combinatorial treatment, mice with mean tumor volumes of 150–200 mm^3 were treated i.p. with two doses of 6 mg/kg DTX on days 1 and 2 of treatment, followed by an i.v. injection of CAR28 T cells (n = 9) or CAR41 T cells (n = 8), respectively, on day 8 of treatment. Control mice were injected with DTX alone (n = 9) or left untreated (control, n = 8). Mice were euthanized at day 22 or earlier, when one of the following termination criteria were met: tumor diameter >15 mm, weight loss >20%, body condition score (BCS) >3, spasms, paralysis, body curvature respiratory disorders, apathy, or aggressiveness.

Histological Analysis

2-μm sections were prepared from formalin-fixed paraffin-embedded tumors and stained with hematoxylin and eosin. Immunohistochemistry was carried out with mouse anti-human CD3 antibody (clone F7.2.38; Dako-Agilent flex kit, Denmark), followed by rabbit anti-

mouse secondary antibody mix, and visualized by an alkaline-based red chromogen reaction (K5005 kit, Dako-Agilent). Images were taken with an Olympus BX 51 microscope (Olympus, Germany) with the AxioCam MRc microscope camera (Carl Zeiss, Germany). For semiquantitative analysis, $CD3^+$ lymphocytes were counted on three ×60 high-power field (HPF) slides (Olympus BX51; ×60/0.9/FN26.5).

Statistical Analysis

Statistical significance in all experiments was determined with the help of GraphPad Prism software by using the unpaired Student's t test.

SUPPLEMENTAL INFORMATION

Supplemental Information can be found online at https://doi.org/10.1016/j.omto.2020.06.014.

AUTHOR CONTRIBUTIONS

T.C., P.W., and H.A. conceived and supervised the study; J.A., J.K., and N.T. carried out the *in vitro* experiments; V.D.-M. and S.T. performed the *in vivo* experiments and the statistical analysis of the data; M.S. performed the histological analyses; S.T., R.Z., W.S., and H.A. provided protocols and advice for the project; J.A., T.C., P.W., and H.A. planned the experiments and interpreted the data; J.A., P.W., and T.C. wrote the manuscript.

CONFLICTS OF INTEREST

Research in the laboratory of T.C. is supported by Cellectis S.A. and Miltenyi Biotec. The remaining authors declare no competing interests.

ACKNOWLEDGMENTS

This work was supported by grants from the Horizon 2020 Programme of the European Commission (CARAT-667980 to T.C.), the German Federal Ministry of Education and Research (IFB-01EO0803 to T.C.), and the Research Commission of the Faculty of Medicine of the Albert-Ludwigs-University of Freiburg (no. WOL1111/16 to P.W. and T.C.). The authors thank Beate vom Hövel for viral vector preparation and Susanne Schultze-Seemann, Irina Kuckuck, and Justin Mastroianni for technical assistance with the experiments, the Lighthouse Core Facility (Medical Center - University of Freiburg) for flow cytometry support, and the Blood Donation Center (Medical Center - University of Freiburg) for providing leukocyte reduction system (LRS) chambers.

REFERENCES

1. Litwin, M.S., and Tan, H.J. (2017). The diagnosis and treatment of prostate cancer: a review. JAMA *317*, 2532–2542.
2. Zhou, C.K., Check, D.P., Lortet-Tieulent, J., Laversanne, M., Jemal, A., Ferlay, J., Bray, F., Cook, M.B., and Devesa, S.S. (2016). Prostate cancer incidence in 43 populations worldwide: an analysis of time trends overall and by age group. Int. J. Cancer *138*, 1388–1400.
3. Zabel, M., Tauber, P.A., and Pickl, W.F. (2019). The making and function of CAR cells. Immunol. Lett. *212*, 53–69.
4. Park, J.H., Rivière, I., Gonen, M., Wang, X., Sénéchal, B., Curran, K.J., Sauter, C., Wang, Y., Santomasso, B., Mead, E., et al. (2018). Long-term follow-up of CD19 CAR therapy in acute lymphoblastic leukemia. N. Engl. J. Med. *378*, 449–459.
5. Maude, S.L., Laetsch, T.W., Buechner, J., Rives, S., Boyer, M., Bittencourt, H., Bader, P., Verneris, M.R., Stefanski, H.E., Myers, G.D., et al. (2018). Tisagenlecleucel in children and young adults with B-cell lymphoblastic leukemia. N. Engl. J. Med. *378*, 439–448.
6. Martinez, M., and Moon, E.K. (2019). CAR T cells for solid tumors: new strategies for finding, infiltrating, and surviving in the tumor microenvironment. Front. Immunol. *10*, 128.
7. Mesters, J.R., Barinka, C., Li, W., Tsukamoto, T., Majer, P., Slusher, B.S., Konvalinka, J., and Hilgenfeld, R. (2006). Structure of glutamate carboxypeptidase II, a drug target in neuronal damage and prostate cancer. EMBO J. *25*, 1375–1384.
8. Wright, G.L., Jr., Grob, B.M., Haley, C., Grossman, K., Newhall, K., Petrylak, D., Troyer, J., Konchuba, A., Schellhammer, P.F., and Moriarty, R. (1996). Upregulation of prostate-specific membrane antigen after androgen-deprivation therapy. Urology *48*, 326–334.
9. Silver, D.A., Pellicer, I., Fair, W.R., Heston, W.D., and Cordon-Cardo, C. (1997). Prostate-specific membrane antigen expression in normal and malignant human tissues. Clin. Cancer Res. *3*, 81–85.
10. Kawakami, M., and Nakayama, J. (1997). Enhanced expression of prostate-specific membrane antigen gene in prostate cancer as revealed by in situ hybridization. Cancer Res. *57*, 2321–2324.
11. Wüstemann, T., Haberkorn, U., Babich, J., and Mier, W. (2019). Targeting prostate cancer: prostate-specific membrane antigen based diagnosis and therapy. Med. Res. Rev. *39*, 40–69.
12. Chang, S.S., Reuter, V.E., Heston, W.D., Bander, N.H., Grauer, L.S., and Gaudin, P.B. (1999). Five different anti-prostate-specific membrane antigen (PSMA) antibodies confirm PSMA expression in tumor-associated neovasculature. Cancer Res. *59*, 3192–3198.
13. Ma, Q., Safar, M., Holmes, E., Wang, Y., Boynton, A.L., and Junghans, R.P. (2004). Anti-prostate specific membrane antigen designer T cells for prostate cancer therapy. Prostate *61*, 12–25.
14. Frigerio, B., Fracasso, G., Luison, E., Cingarlini, S., Mortarino, M., Coliva, A., Seregni, E., Bombardieri, E., Zuccolotto, G., Rosato, A., et al. (2013). A single-chain fragment against prostate specific membrane antigen as a tool to build theranostic reagents for prostate cancer. Eur. J. Cancer *49*, 2223–2232.
15. Wolf, P., Freudenberg, N., Bühler, P., Alt, K., Schultze-Seemann, W., Wetterauer, U., and Elsässer-Beile, U. (2010). Three conformational antibodies specific for different PSMA epitopes are promising diagnostic and therapeutic tools for prostate cancer. Prostate *70*, 562–569.
16. Stephan, M.T., Ponomarev, V., Brentjens, R.J., Chang, A.H., Dobrenkov, K.V., Heller, G., and Sadelain, M. (2007). T cell-encoded CD80 and 4-1BBL induce auto- and transcostimulation, resulting in potent tumor rejection. Nat. Med. *13*, 1440–1449.
17. Zhong, X.S., Matsushita, M., Plotkin, J., Riviere, I., and Sadelain, M. (2010). Chimeric antigen receptors combining 4-1BB and CD28 signaling domains augment PI3kinase/AKT/Bcl-X_L activation and $CD8^+$ T cell-mediated tumor eradication. Mol. Ther. *18*, 413–420.
18. Ma, Q., Gomes, E.M., Lo, A.S., and Junghans, R.P. (2014). Advanced generation anti-prostate specific membrane antigen designer T cells for prostate cancer immunotherapy. Prostate *74*, 286–296.
19. Santoro, S.P., Kim, S., Motz, G.T., Alatzoglou, D., Li, C., Irving, M., Powell, D.J., Jr., and Coukos, G. (2015). T cells bearing a chimeric antigen receptor against prostate-specific membrane antigen mediate vascular disruption and result in tumor regression. Cancer Immunol. Res. *3*, 68–84.
20. Gade, T.P., Hassen, W., Santos, E., Gunset, G., Saudemont, A., Gong, M.C., Brentjens, R., Zhong, X.S., Stephan, M., Stefanski, J., et al. (2005). Targeted elimination of prostate cancer by genetically directed human T lymphocytes. Cancer Res. *65*, 9080–9088.
21. Zuccolotto, G., Fracasso, G., Merlo, A., Montagner, I.M., Rondina, M., Bobisse, S., Figini, M., Cingarlini, S., Colombatti, M., Zanovello, P., and Rosato, A. (2014). PSMA-specific CAR-engineered T cells eradicate disseminated prostate cancer in preclinical models. PLoS ONE *9*, e109427.

22. Ristau, B.T., O'Keefe, D.S., and Bacich, D.J. (2014). The prostate-specific membrane antigen: lessons and current clinical implications from 20 years of research. Urol. Oncol. *32*, 272–279.

23. Junghans, R.P., Ma, Q., Rathore, R., Gomes, E.M., Bais, A.J., Lo, A.S., Abedi, M., Davies, R.A., Cabral, H.J., Al-Homsi, A.S., and Cohen, S.I. (2016). Phase I trial of anti-PSMA designer CAR-T cells in prostate cancer: possible role for interacting interleukin 2-T cell pharmacodynamics as a determinant of clinical response. Prostate *76*, 1257–1270.

24. Narayan, V., Gladney, W., Plesa, G., Vapiwala, N., Carpenter, E., Maude, S.L., Lal, P., Lacey, S.F., Melenhorst, J.J., Sebro, R., et al. (2019). A phase I clinical trial of PSMA-directed/TGFβ-insensitive CAR-T cells in metastatic castration-resistant prostate cancer. J. Clin. Oncol. *37* (*Suppl*), TPS347.

25. Kloss, C.C., Lee, J., Zhang, A., Chen, F., Melenhorst, J.J., Lacey, S.F., Maus, M.V., Fraietta, J.A., Zhao, Y., and June, C.H. (2018). Dominant-negative TGF-β receptor enhances PSMA-targeted human CAR T cell proliferation and augments prostate cancer eradication. Mol. Ther. *26*, 1855–1866.

26. Michalska, M., Schultze-Seemann, S., Bogatyreva, L., Hauschke, D., Wetterauer, U., and Wolf, P. (2016). In vitro and in vivo effects of a recombinant anti-PSMA immunotoxin in combination with docetaxel against prostate cancer. Oncotarget *7*, 22531–22542.

27. Michalska, M., Schultze-Seemann, S., Kuckuck, I., and Wolf, P. (2018). *In vitro* evaluation of humanized/de-immunized anti-PSMA immunotoxins for the treatment of prostate cancer. Anticancer Res. *38*, 61–69.

28. Baum, V., Bühler, P., Gierschner, D., Herchenbach, D., Fiala, G.J., Schamel, W.W., Wolf, P., and Elsässer-Beile, U. (2013). Antitumor activities of PSMA×CD3 diabodies by redirected T-cell lysis of prostate cancer cells. Immunotherapy *5*, 27–38.

29. Fortmüller, K., Alt, K., Gierschner, D., Wolf, P., Baum, V., Freudenberg, N., Wetterauer, U., Elsässer-Beile, U., and Bühler, P. (2011). Effective targeting of prostate cancer by lymphocytes redirected by a PSMA × CD3 bispecific single-chain diabody. Prostate *71*, 588–596.

30. Wolf, P., Alt, K., Wetterauer, D., Bühler, P., Gierschner, D., Katzenwadel, A., Wetterauer, U., and Elsässer-Beile, U. (2010). Preclinical evaluation of a recombinant anti-prostate specific membrane antigen single-chain immunotoxin against prostate cancer. J. Immunother. *33*, 262–271.

31. Bühler, P., Molnar, E., Dopfer, E.P., Wolf, P., Gierschner, D., Wetterauer, U., Schamel, W.W., and Elsässer-Beile, U. (2009). Target-dependent T-cell activation by coligation with a PSMA×CD3 diabody induces lysis of prostate cancer cells. J. Immunother. *32*, 565–573.

32. Gao, Q., Wang, S., Chen, X., Cheng, S., Zhang, Z., Li, F., Huang, L., Yang, Y., Zhou, B., Yue, D., et al. (2019). Cancer-cell-secreted CXCL11 promoted $CD8^+$ T cells infiltration through docetaxel-induced-release of HMGB1 in NSCLC. J. Immunother. Cancer *7*, 42.

33. Haso, W., Lee, D.W., Shah, N.N., Stetler-Stevenson, M., Yuan, C.M., Pastan, I.H., Dimitrov, D.S., Morgan, R.A., FitzGerald, D.J., Barrett, D.M., et al. (2013). Anti-CD22-chimeric antigen receptors targeting B-cell precursor acute lymphoblastic leukemia. Blood *121*, 1165–1174.

34. Ying, Z., Huang, X.F., Xiang, X., Liu, Y., Kang, X., Song, Y., Guo, X., Liu, H., Ding, N., Zhang, T., et al. (2019). A safe and potent anti-CD19 CAR T cell therapy. Nat. Med. *25*, 947–953.

35. Feucht, J., Sun, J., Eyquem, J., Ho, Y.J., Zhao, Z., Leibold, J., Dobrin, A., Cabriolu, A., Hamieh, M., and Sadelain, M. (2019). Calibration of CAR activation potential directs alternative T cell fates and therapeutic potency. Nat. Med. *25*, 82–88.

36. Hombach, A., Hombach, A.A., and Abken, H. (2010). Adoptive immunotherapy with genetically engineered T cells: modification of the IgG1 Fc "spacer" domain in the extracellular moiety of chimeric antigen receptors avoids 'off-target' activation and unintended initiation of an innate immune response. Gene Ther. *17*, 1206–1213.

37. Kofler, D.M., Chmielewski, M., Rappl, G., Hombach, A., Riet, T., Schmidt, A., Hombach, A.A., Wendtner, C.M., and Abken, H. (2011). CD28 costimulation Impairs the efficacy of a redirected T-cell antitumor attack in the presence of regulatory T cells which can be overcome by preventing Lck activation. Mol. Ther. *19*, 760–767.

38. van der Stegen, S.J., Hamieh, M., and Sadelain, M. (2015). The pharmacology of second-generation chimeric antigen receptors. Nat. Rev. Drug Discov. *14*, 499–509.

39. Zhang, Z., Jiang, D., Yang, H., He, Z., Liu, X., Qin, W., Li, L., Wang, C., Li, Y., Li, H., et al. (2019). Modified CAR T cells targeting membrane-proximal epitope of mesothelin enhances the antitumor function against large solid tumor. Cell Death Dis. *10*, 476.

40. Bander, N.H., Nanus, D.M., Milowsky, M.I., Kostakoglu, L., Vallabahajosula, S., and Goldsmith, S.J. (2003). Targeted systemic therapy of prostate cancer with a monoclonal antibody to prostate-specific membrane antigen. Semin. Oncol. *30*, 667–676.

41. Schmidts, A., and Maus, M.V. (2018). Making CAR T cells a solid option for solid tumors. Front. Immunol. *9*, 2593.

42. Bobisse, S., Rondina, M., Merlo, A., Tisato, V., Mandruzzato, S., Amendola, M., Naldini, L., Willemsen, R.A., Debets, R., Zanovello, P., and Rosato, A. (2009). Reprogramming T lymphocytes for melanoma adoptive immunotherapy by T-cell receptor gene transfer with lentiviral vectors. Cancer Res. *69*, 9385–9394.

43. Cornu, T.I., Mussolino, C., and Cathomen, T. (2017). Refining strategies to translate genome editing to the clinic. Nat. Med. *23*, 415–423.

44. Mussolino, C., Alzubi, J., Pennucci, V., Turchiano, G., and Cathomen, T. (2017). Genome and epigenome editing to treat disorders of the hematopoietic system. Hum. Gene Ther. *28*, 1105–1115.

45. Menger, L., Sledzinska, A., Bergerhoff, K., Vargas, F.A., Smith, J., Poirot, L., Pule, M., Hererro, J., Peggs, K.S., and Quezada, S.A. (2016). TALEN-mediated inactivation of PD-1 in tumor-reactive lymphocytes promotes intratumoral T-cell persistence and rejection of established tumors. Cancer Res. *76*, 2087–2093.

46. Ren, J., Liu, X., Fang, C., Jiang, S., June, C.H., and Zhao, Y. (2017). Multiplex genome editing to generate universal CAR T cells resistant to PD1 inhibition. Clin. Cancer Res. *23*, 2255–2266.

47. Zhang, Y., Zhang, X., Cheng, C., Mu, W., Liu, X., Li, N., Wei, X., Liu, X., Xia, C., and Wang, H. (2017). CRISPR-Cas9 mediated LAG-3 disruption in CAR-T cells. Front. Med. *11*, 554–562.

48. Poirot, L., Philip, B., Schiffer-Mannioui, C., Le Clerre, D., Chion-Sotinel, I., Derniame, S., Potrel, P., Bas, C., Lemaire, L., Galetto, R., et al. (2015). Multiplex genome-edited T-cell manufacturing platform for "off-the-shelf" adoptive T-cell immunotherapies. Cancer Res. *75*, 3853–3864.

49. Dürr, C., Pfeifer, D., Claus, R., Schmitt-Graeff, A., Gerlach, U.V., Graeser, R., Krüger, S., Gerbitz, A., Negrin, R.S., Finke, J., and Zeiser, R. (2010). CXCL12 mediates immunosuppression in the lymphoma microenvironment after allogeneic transplantation of hematopoietic cells. Cancer Res. *70*, 10170–10181.

50. Dettmer, V., Bloom, K., Gross, M., Weissert, K., Aichele, P., Ehl, S., and Cathomen, T. (2019). Retroviral *UNC13D* gene transfer restores cytotoxic activity of T cells derived from familial hemophagocytic lymphohistiocytosis type 3 patients *in vitro*. Hum. Gene Ther. *30*, 975–984.

51. Bobis-Wozowicz, S., Galla, M., Alzubi, J., Kuehle, J., Baum, C., Schambach, A., and Cathomen, T. (2014). Non-integrating gamma-retroviral vectors as a versatile tool for transient zinc-finger nuclease delivery. Sci. Rep. *4*, 4656.

52. Golumba-Nagy, V., Kuehle, J., and Abken, H. (2017). Genetic modification of T cells with chimeric antigen receptors: a laboratory manual. Hum. Gene Ther. Methods *28*, 302–309.

53. Koehler, H., Kofler, D., Hombach, A., and Abken, H. (2007). CD28 costimulation overcomes transforming growth factor-β-mediated repression of proliferation of redirected human $CD4^+$ and $CD8^+$ T cells in an antitumor cell attack. Cancer Res. *67*, 2265–2273.

OMTO, Volume *18*

Supplemental Information

PSMA-Directed CAR T Cells Combined with Low-Dose Docetaxel Treatment Induce Tumor Regression in a Prostate Cancer Xenograft Model

Jamal Alzubi, Viviane Dettmer-Monaco, Johannes Kuehle, Niko Thorausch, Maximilian Seidl, Sanaz Taromi, Wolfgang Schamel, Robert Zeiser, Hinrich Abken, Toni Cathomen, and Philipp Wolf

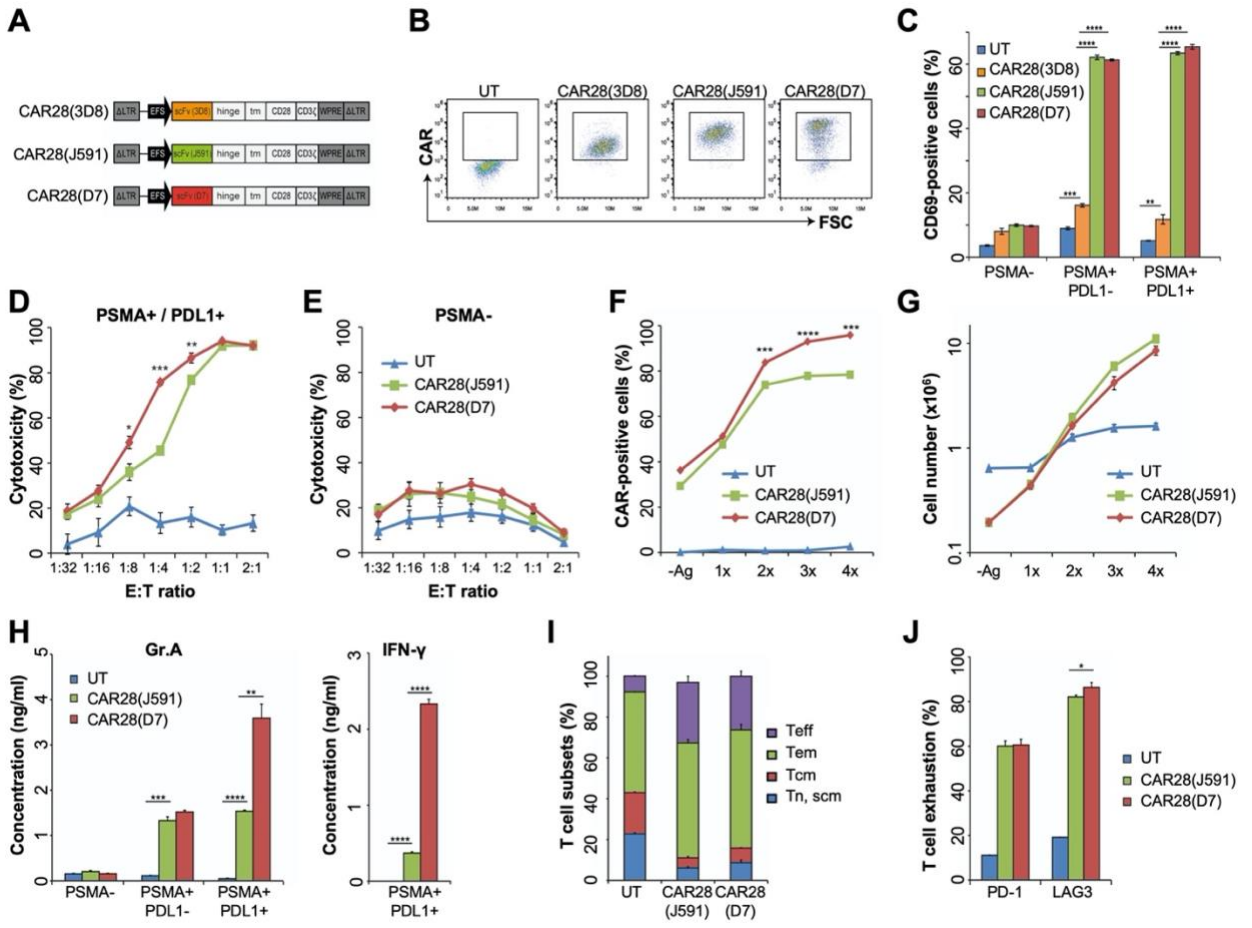

Figure S1. Characterization of PSMA-CARs. (A) Schematic of γ-retroviral vectors. CAR expression is driven by an EFS promoter. The CARs consist of a single chain variable (scFv) fragment derived from 3D8, J591 or D7 antibodies, respectively, a hinge region (modified Fc IgG1 domain), a transmembrane domain, a costimulatory domain derived from CD28 with a mutated LcK binding moiety, and an intracellular signaling domain derived from CD3ζ chain. **(B)** CAR expression. Jurkat cells were transduced with retroviral particles, followed by expansion and staining with anti-human IgG antibody. (**C**) PSMA-mediated activation of CAR expressing Jurkat cells. Cells were co-cultured at a 1:1 effector-to-target (E:T) ratio with either C4-2 (PSMA-positive/PDL1-negative) or LNCap (PSMA-positive/PDL1-positive) tumor cells. PSMA-negative DU145 cells served as control. Activation was assessed by evaluating the percentage of CD69 positive cells (n=3). (**D-E**) Cytolytic activity. CAR T cells were co-cultured at indicated E:T ratios with either LNCaP (D) or DU145 (E) tumor cells. Cytotoxicity was determined by cell viability assay (% cytotoxicity = 100 – % viability). (**F-G**) Antigen-specific CAR T cell proliferation. CAR T cells were propagated without antigen stimulation (-Ag) or exposed to irradiated PSMA-positive C4-2 cells up to 4 times (1–4x) at E:T ratios of 1:1. Cells were stained with CD3 and anti-human IgG (CAR) antibodies to determine the fraction of CAR-positive cells (F) or the total number of CAR-positive cells (G). (**H**) Granzyme and cytokine release. Untransduced or CAR T cells were co-cultured at a 1:1 effector-to-target (E:T) ratio with either C4-2 (PSMA-positive/PDL1-negative) or LNCap (PSMA-positive/PDL1-positive) tumor cells. PSMA-negative DU145 cells served as control. Granzyme A (Gr.A) or IFNγ concentration in supernatant was quantified by cytometric bead array (n=3). (**I-J**) Untransduced T cells (UT) or CAR T cells were co-cultured at a 1:1 E:T ratio with C4-2 cells. (**I**) CAR T cell phenotype. Shown are the percentages of T cell subsets (n=3) based on CD62L and CD45RA expression. (**J**) CAR T cell exhaustion. Shown are the percentages of PD-1 or LAG3 positive cells (n=3). Cells were pre-gated on CD3 for UT, or CD3/CAR for CAR T cells. Statistically significant differences are indicated by *(P<0.05), **(P<0.01), ***(P<0.001), or ****(P<0.0001). UT, untransduced T cells; PDL1, programmed cell death ligand 1; ΔLTR, long-terminal repeat with deletion in U3 region; EFS, elongation factor 1α short promoter; WPRE, woodchuck hepatitis virus post-transcriptional regulatory element; Tn/Tscm, T cell naïve or T stem cell memory; Tcm, T cell central memory; Tem, T cell effector memory; Teff, T cell effector.

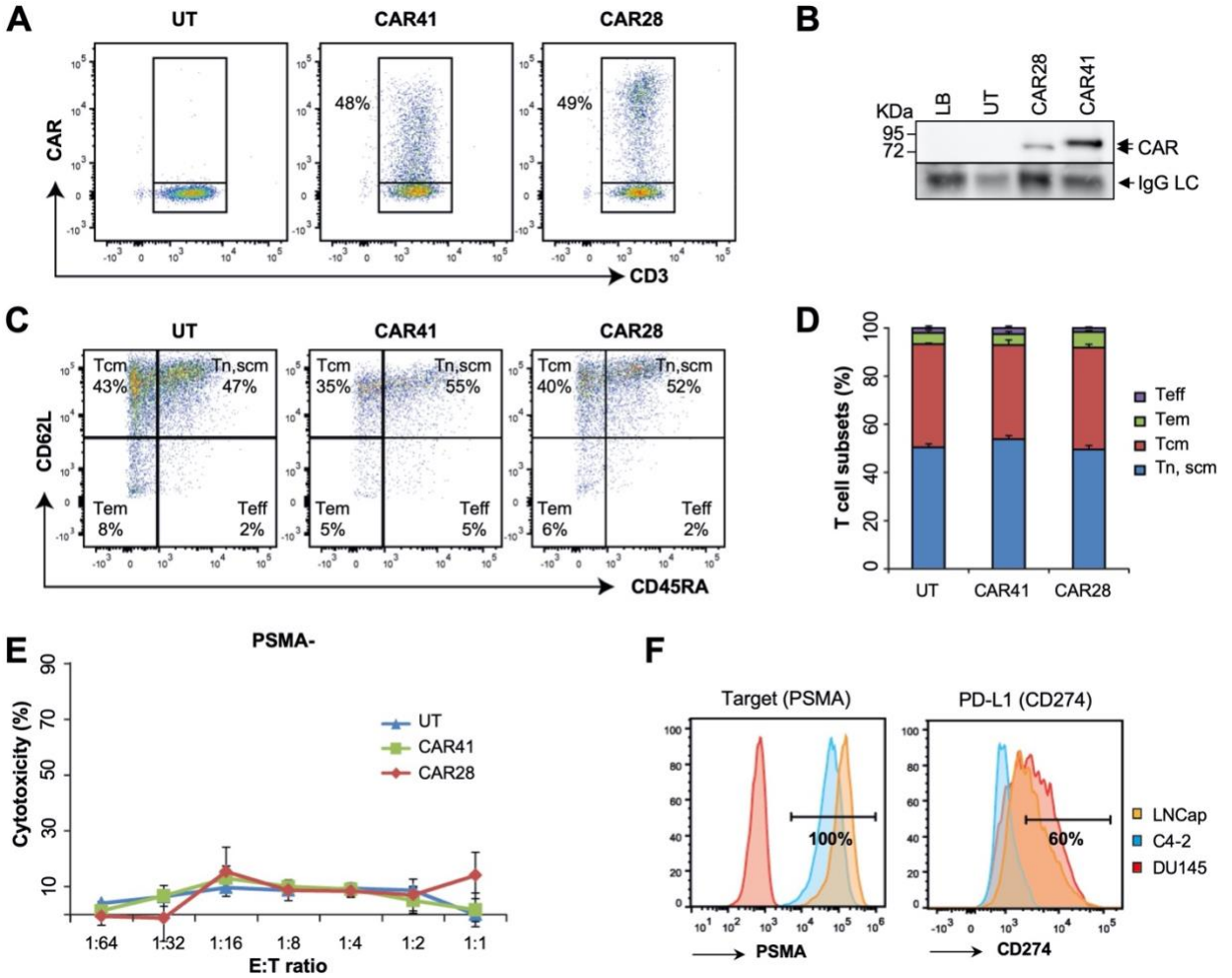

Figure S2. Quality assessment. (A) Evaluation of CAR surface expression. After transduction of activated T cells with γ-retroviral vectors, CAR T cell were expanded and stained with antibodies against anti-human IgG (CAR) and CD3. **(B)** CAR expression. CAR T cells were lysed, CARs immune-precipitated using anti-scFv antibody, and CAR expression visualized by Western blot analysis. Anti-IgG antibody staining served as a loading control. **(C)** CAR T cell phenotyping. The percentages of T cell subsets were determined at the end of the expansion phase by assessing the expression of CD62L and CD45RA by flow cytometry. Cells were pre-gated on CAR-/CD3+ for the UT or CAR+/CD3+ for of CAR T cells. **(D)** Quantitative assessment of CAR T cell phenotypes. Shown are the average percentages of T cell subsets (n=3 or 4). **(E)** Cytolytic activity. CAR T cells were co-cultured at indicated effector to target (E:T) ratios with PSMA-negative DU145 tumor cells. Cytotoxicity was determined by cell viability assay (% cytotoxicity = 100 – % viability). (**F**) Characterization of Prostate cancer cell lines. Cells were stained with anti-PSMA (3/F11) and CD274 (PD-L1) antibodies, respectively, and expression levels assessed by flow cytometry. PSMA, prostate-specific membrane antigen; PD-L1, programmed cell death ligand 1; LB, lysis buffer; UT, untransduced T cells; IgG LC, IgG light chain loading control; Tn/Tscm, T cell naïve or T stem cell memory; Tcm, T cell central memory; Tem, T cell effector memory; Teff, T cell effector.

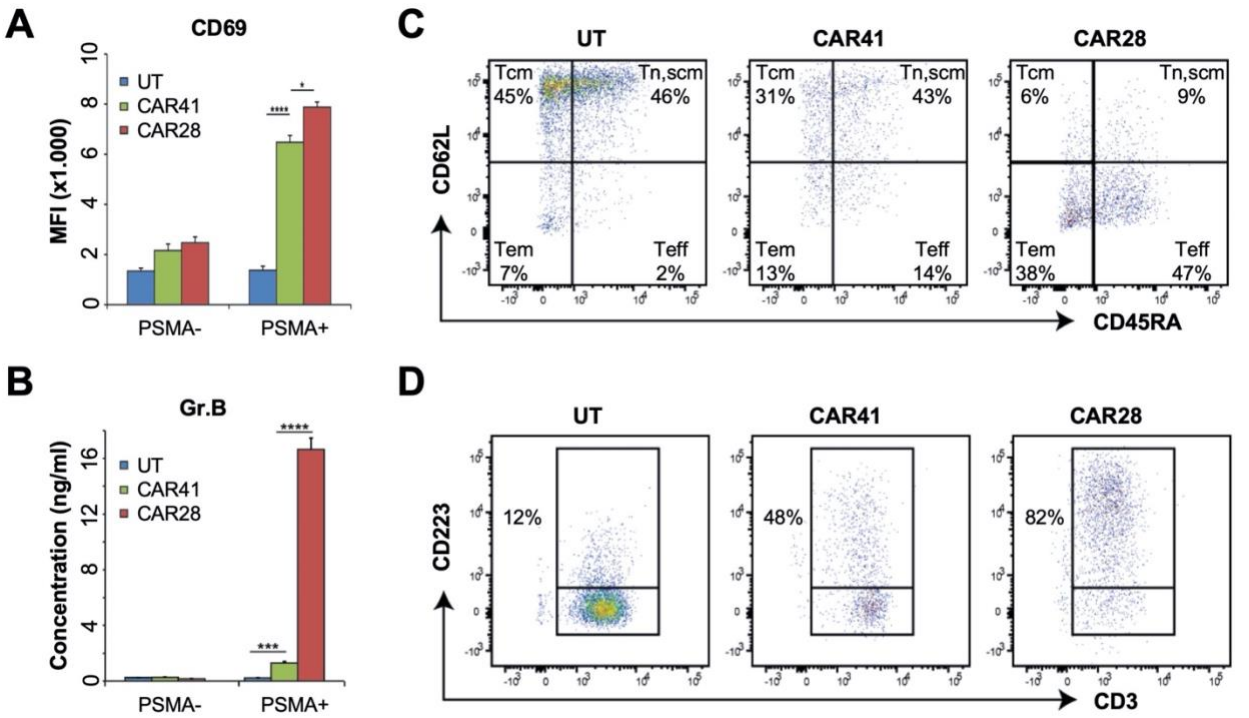

Figure S3. Extended phenotypic and functional analysis of PSMA-targeting CAR T cells. Untransduced T cells (UT), CAR41 or CAR28 T cells were co-cultured with PSMA-positive (C4-2) or PSMA-negative (Du145) tumor cells at a 1:1 effector-to-target (E:T) ratio. (**A**) PSMA-mediated activation. CAR T cell activation was assessed by evaluating CD69 expression. Indicated is mean fluorescent intensity (MFI, n=6). (**B**) Granzyme release. Granzyme B (Gr.B) concentration in supernatant was quantified by cytometric bead array (n=3). (**C**) Phenotype. CAR T cell phenotypes were assessed based on CD62L and CD45RA expression. Cells were pre-gated on either CD3 alone for UT control, or CAR and CD3 for CAR T cells. (**D**) CAR T cell exhaustion. Extent of exhaustion was assessed by measuring CD223 (LAG-3) expression. Cells were pre-gated on CD3 alone for UT control, or CAR and CD3 for CAR T cells. Statistically significant differences are indicated by *(P<0.05), ***(P<0.001), or ****(P<0.0001). Tn/Tscm, T cell naïve or T stem cell memory; Tcm, T cell central memory; Tem, T cell effector memory; Teff, T cell effector.

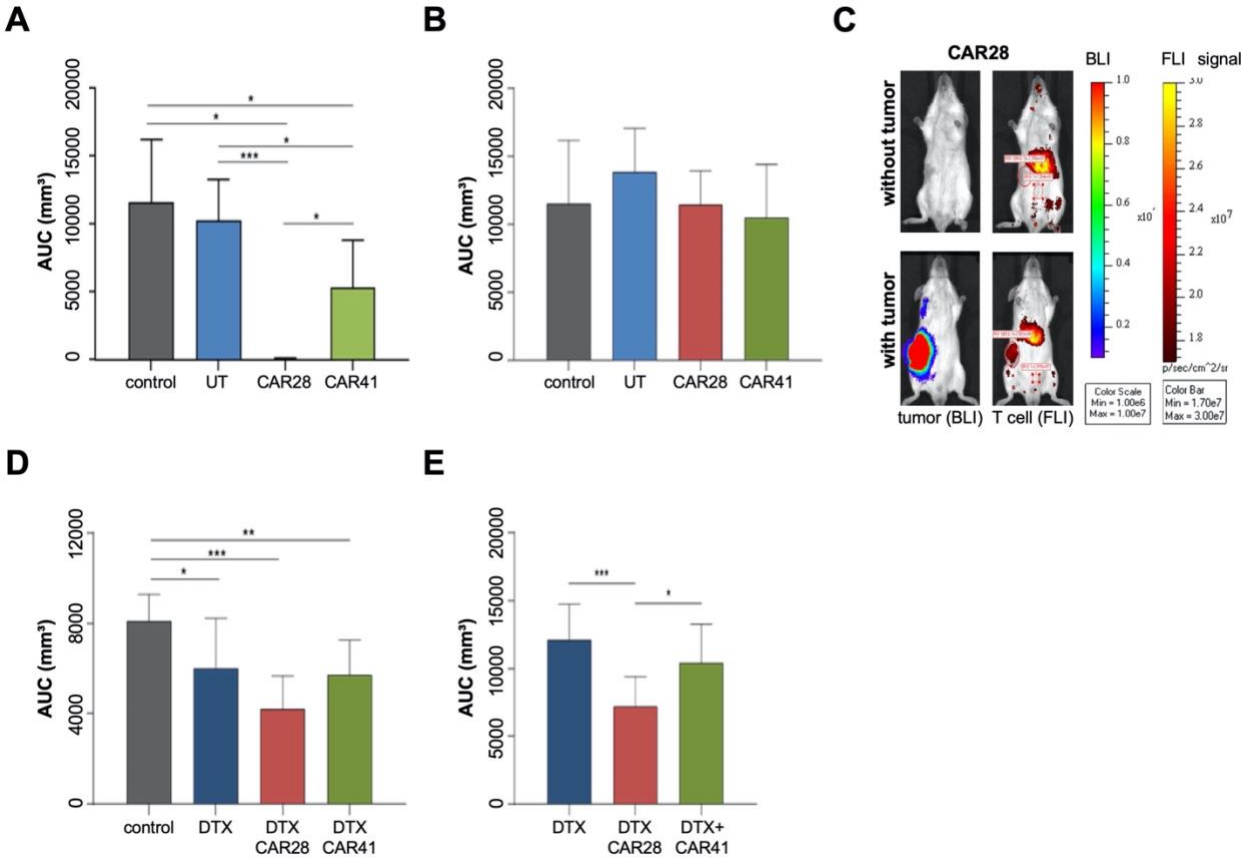

Figure S4. Therapy response of mice bearing human prostate tumors xenografts. Antitumor activity of anti-PSMA CAR T cells upon focal **(A)** or systemic application **(B)**. One dose of $5x10^6$ D7-based CAR28 or CAR41 T cells were injected either intratumorally (A) or intravenously (B). Tumor volumes from individual groups were monitored by calculating the area under the curve (AUC) over the entire course of the experiment, starting from day 1 of the therapy until the end at day 22. As controls, mice were left untreated (control) or treated with untransduced T cells (UT). **(C)** Biodistribution of anti-PSMA CAR28 T cells. CAR T cells were labelled with Xenolight DiR dye and injected intravenously into mice bearing PSMA-positive tumor xenografts or controls without tumor. 24 hours post-infusion, tumors were monitored by *in vivo* bioluminescence imaging (BLI) while labeled T cells were detected by fluorescence imaging (FLI). (**D**-**E**) Anti-tumor activity of combined therapy with DTX and anti-PSMA CAR T cells. Mice bearing tumors of ~150-200 mm^3 were treated with 2 cycles of docetaxel (DTX) followed by intravenous injection of $5x10^6$ CAR28 (n=9) or CAR41 T cells (n=8). As controls, mice were treated with DTX alone (n=9) of left untreated (control, n=8). Changes in tumor volumes from individual treated groups were monitored by calculating the AUC over the course of the entire experiment, starting from day 1 of the therapy until day 17 (D) or until the end of the therapy at day 22 (E). Statistically significant differences were determined by unpaired t-test: *p<0.05, **p<0.01 and ***p<0.001.

Supplemental Methods

Western blot

To verify the size of our CAR28 or CAR41, we have performed Immuno-purification and western blotting of chimeric antigen receptors from cellular lysates as previously described (REF: PMID 31064990). Briefly, 3×10^7 cells were lysed in 1 ml lysis buffer containing 20 mM Tris-HCl pH8, 137 mM NaCl, 2 mM EDTA, 10% glycerol, 1x protease inhibitor cocktail, 1 mM PMSF, 5 mM iodoacetamide, 0.5 mM sodium orthovanadate, 1 mM NaF, and 0.5% Brij96 for 30 min at 4 °C followed by 15 min centrifugation to pellet the nuclei and insoluble material. For immuno-purification of the chimeric antigen receptors, 400 µl cleared cell lysate was incubated with 7.5 µl streptavidin-coupled sepharose (#17-5113-01, GE Healtcare) and 20 µg biotin-coupled anti-mouse IgG (Fab´)2 biotin (#31803, ThermoFisher) for 2 h at 4 °C. After four washes, the immunoprecipitated material was separated by 12% reducing SDS-PAGE. The separated proteins were transferred to PVDF membranes by semi-dry transfer. After blocking with 5% milk in PBS containing 0.1% Tween-20 the membranes were incubated with HRPO-conjugated secondary antibodies (1:10000) (anti-rabbit IgG HRPO, #31460, ThermoFisher). Western blot signals were recorded using an Image Quant LAS 4000 Mini from GE Healthcare Life Sciences, Boston, MA.

Phenotyping of prostate cancer cells

To evaluate PSMA expression, cells were incubated with 2.8 µg/ml anti-PSMA mAb 3/F11 for 30 minutes at 4°C followed by staining with a 1:100 dilution of goat anti-mouse Ig-PE (Southern Biotech) for 30 minutes in dark at 4°C and evaluation by flow cytometery. To determine PD-L1 expression, prostate cancer cells were stained with anti-CD274-Bv421 (Biolegend) and evaluated by flow cytometery.

In vivo biodistribution of CAR T cells

In order to track CAR T cells in vivo, cells were labelled with Xenolight DiR dye (Caliper LifeSciences) according to the manufacturer's recommendations. Shortly, $2\text{-}3x10^6$ cells/ml of RPMI medium supplemented with 0.1% FCS were labelled with a 1:500 dilution of DiR (8.3 mg/ml) for 10 min. at 37°C. Then, cells were washed 3 times before i.v. injection into tumor bearing mice. After 24 h, mice were imaged under anesthesia using the In Vivo Imaging System IVIS 200 (Xenogen VivoVision) in the FLI channel.

Antigen-specific expansion of PSMA-targeting CAR T cells

CAR T cells were generated from PBMCs following retroviral transduction as described in Materials and Methods. At day 12 post-transduction, CAR T cells were co-cultured with irradiated PSMA-positive C4-2 tumor cells for 12 days at a 1:1 effector-to-target ratio in RPMI complete medium supplemented with 100 U/ml of IL-2, 25 U/ml of IL-7, and 50 U/ml of IL-15 (all Miltenyi Biotech). Every 3 days, cells were harvested, counted and plated over fresh irradiated C4-2 tumor cells. Cells were stained with anti-human IgG-PE (Southern Biotech) and anti-CD3-APC (Miltenyi) antibodies to determine CAR expression levels and the fraction of CAR-positive cells by flow cytometry (Accuri, BD Biosciences). The absolute number of CAR T cells was determined at indicated time points using a NucleoCounter (NC-250, ChemoMetec).